

Tuning Hole Mobility, Concentration, and Repulsion in High- T_c Cuprates via Apical Atoms

Wei-Guo Yin¹ and Wei Ku^{1,2}

¹Condensed Matter Physics & Materials Science Department, Brookhaven National Laboratory, Upton, NY 11973

²Physics Department, State University of New York, Stony Brook, NY 11790

(Dated: Received June 9, 2018)

Using a newly developed first-principles Wannier-states approach that takes into account large on-site Coulomb repulsion, we derive the effective low-energy interacting Hamiltonians for several prototypical high- T_c superconducting cuprates. The material dependence is found to originate primarily from the different energy of the apical atom p_z state. Specifically, the general properties of the low-energy hole state, namely the Zhang-Rice singlet, are significantly modified by a triplet state associated with this p_z state, via additional intra-sublattice hoppings, nearest-neighbor “super-repulsion”, and other microscopic many-body processes. Possible implications on modulation of T_c , local superconducting gaps, charge distribution, hole mobility, electron-phonon interaction, and multi-layer effects are discussed.

PACS numbers: 74.72.-h, 71.10.-w, 74.25.Jb, 74.40.+k

Introduction.—The origin of high- T_c superconductivity (HTSC) remains under fierce debate notwithstanding monumental effort for two decades [1]. This fascinating phenomenon is achieved when a number of layered copper oxides are doped away from their Mott insulating parent phase. Although it is generally agreed that the most relevant electron behavior is confined within the common $(\text{CuO}_2)^{2-}$ plane, T_c^{max} (T_c at optimal doping) strikingly varies from 28 K in $\text{Ca}_{2-x}\text{Na}_x\text{CuO}_2\text{Cl}_2$ to 135 K in $\text{HgBa}_2\text{Ca}_2\text{Cu}_3\text{O}_{8+\delta}$ by modulation of the layering pattern along the less essential third direction. Hence, clarifying the material dependence of the in-plane electron behavior, especially in unbiased first-principles-based approaches, is an essential and effective step toward the resolution of the HTSC mechanism and the quest for higher T_c superconductors.

A recent influential advancement along the line was made by Andersen and coworkers [2]. Within the local-density approximation (LDA) of density-functional theory, they derived a one-band *noninteracting* Hamiltonian for several hole-doped cuprates, showing that $-t'/t$ (t and t' are the first- and second-nearest-neighbor hopping integrals, respectively) was strongly material-dependent and correlated with T_c^{max} . Taken as the kinetic part of the effective one-band t - J or Hubbard model, the most studied model for the CuO_2 plane [3], this single band has been widely used to compare with angular-resolved photoemission spectroscopy (ARPES) [4, 5, 6].

A particular puzzle thus caused is that the LDA results of $-t'/t = 0.18$ for La_2CuO_4 and 0.12 for $\text{Ca}_2\text{CuO}_2\text{Cl}_2$ [2] are in striking contradiction to their diamond- and square-like Fermi surfaces, respectively, as observed in ARPES [4, 5]. In addition, the low-energy carriers in hole-doped cuprates are well accepted to be closely related to the Zhang-Rice singlet (ZRS) that naturally appears in deriving the t - J model from an interacting many-body picture [7]. This two-body singlet state is *intrinsically different* from any single-particle state. Therefore, it is essential to reexamine the material dependence by moving one step forward to derive an effective *interacting* Hamiltonian in a first-principles approach that takes into account, from the beginning, the large Coulomb repulsion on the

Cu sites. New material-dependent interaction effects are then expected to be revealed from the strong electronic interaction and the charge-transfer nature [8].

In this Letter, using a recently developed first-principles Wannier-states (WSs) approach [9, 10] which takes into account large on-site Coulomb repulsion, we derive the effective low-energy interacting Hamiltonians for several prototypical high- T_c superconducting cuprates. The only significant microscopic difference among the cuprates is found to originate from the apical atom p_z state. Strong impact of the apical atom on t' is observed; in particular, $-t'/t$ for $\text{Ca}_2\text{CuO}_2\text{Cl}_2$ is found to be considerably larger than for La_2CuO_4 , in good agreement with ARPES. Moreover, we show that besides the t' and electrostatic effects, the realistic variation of the energy level of the apical p_z states is able to tune substantially the local site potential and intersite “super-repulsion,” directly modulating the local superconducting gap and charge distribution. This provides a natural explanation of recent spectroscopic imaging scanning tunneling microscopy (SI-STM) observations [11, 12]. Finally, implication on a new realization of the electron-phonon coupling is briefly addressed. These important findings should shed new light on the general material dependence and microscopic understanding of HTSC.

Methods.—A three-step approach is employed to systematically reduce the energy scale of the relevant Hilbert space: (i) The full-energy electronic structures are obtained within the LDA+ U approximation [13] known as a state-of-the-art generalization of LDA to include strong local interaction. (ii) At the intermediate-energy scale (~ 10 eV covering the Cu $3d$, O $2p$, and relevant apical orbitals), an effective five-band interacting Hamiltonian, H^{5b} , is derived [9]. The local part of H^{5b} , which includes the leading terms (on-Cu-site interaction and local d - p hybridization), is then diagonalized for all the doping levels [14, 15, 16]. (iii) At the low-energy scale (~ 1 eV), an effective one-band Hamiltonian, H^{1b} , is derived from canonical transformation to project out high-energy states up to the second order [16].

Since the apical (out-of-plane) coordination of the planar Cu cations is the main structural variation relevant to the

physics of the CuO_2 plane, we present here a study of a number of cuprates representing different apical limits: La_2CuO_4 with two apical oxygen atoms per copper site, $\text{Ca}_2\text{CuO}_2\text{Cl}_2$ with the apical p_z energy level, ε_{P_z} , moved away from the Fermi level by substitution of Cl for O, $\text{Sr}_2\text{CuO}_2\text{F}_2$ with ε_{P_z} moved farther away, and Nd_2CuO_4 without apical atoms (equivalently, $\varepsilon_{P_z} = \infty$).

The most relevant WFs are shown in Fig. 1(a), including the Cu $3d$, O $2p$, and apical p orbitals, spanning an energy window of ~ 10 eV [c.f. Fig. 1(b)]. Since these WFs almost completely decouple from other WFs, a five-band Hamiltonian H^{5b} with on-site Coulomb and exchange interactions among the Cu $d_{x^2-y^2}$ and $d_{3z^2-r^2}$ orbitals can be unambiguously derived by matching its self-consistent Hartree-Fock expression with the Wannier representation of the LDA+ U Hamiltonian [9]. The details will be presented elsewhere. Indeed, among the cuprates, the most noticeable difference in the parameters of H^{5b} is ε_{P_z} [17], as presented in Table I.

The likelihood of a one-band picture is readily revealed by our WFs analysis of the LDA+ U band. Fig. 1(b) shows such an analysis for $\text{Ca}_2\text{CuO}_2\text{Cl}_2$, for there exist excellent ARPES data to compare with. Note that the lowest unoccupied band is mainly of Cu $3d_{x^2-y^2}$ character and the highest occupied band is mainly of O P_s character. Apparently, these two in-plane bands are the most relevant to the low-energy physics; indeed, their overall shapes agree well with the ARPES [4]. In addition, their corresponding WFs have opposite spin characters, as clearly shown in the right panel of Fig. 1(b). Thus,

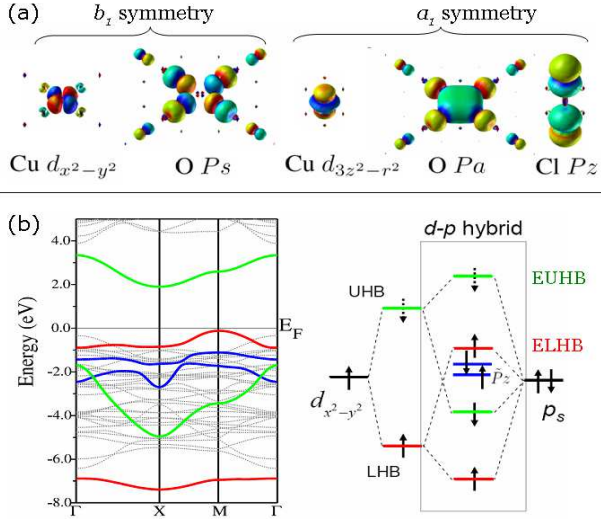


FIG. 1: (Color online) (a) Wannier functions centered at Cu sites for H^{5b} : $O P_s$ and P_a are constructed by maximizing the weight of the b_1 - and a_1 -symmetrized combination of four neighboring planar O p_σ orbitals, respectively; P_z is the a_1 -symmetrized combination of two apical p_z orbitals. (b) Left panel: Band structures of $\text{Ca}_2\text{CuO}_2\text{Cl}_2$ from LDA+ U calculations (dots) and Wannier states analysis (lines). $\Gamma=(0,0,0)$, $X=(\pi,0,0)$, $M=(\frac{\pi}{2},\frac{\pi}{2},0)$. Right panel: Corresponding local energy level splitting due to interactions and d - p hybridization, filled with electrons (solid arrows) or holes (dashed arrows). \tilde{P}_z are derived from two highest a_1 hybrids.

the simplest one-band picture is to view these two anti-spin-polarized bands (both are antibonding between Cu $3d_{x^2-y^2}$ and O P_s WFs) as the effective upper and lower Hubbard bands (EUHB and ELHB) with the charge-transfer gap as the effective Hubbard gap.

A more appropriate approach is to project out high-energy states systematically, based on exact diagonalization of the leading terms (here the local part of H^{5b}) [14, 15, 16]. Specifically, our approach benefits greatly from having all the first-principles WFs, including the O $2p$ states, centered at the Cu sites [see Fig. 1(a)] by construction. This reduces the decorated CuO_2 lattice to a simple square lattice, and unambiguously defines the local Hamiltonian to be diagonalized.

It is appropriate to keep in the low-energy space only the local one-hole and two-hole ground states, referred to as $|\sigma\rangle$ and $|\text{ZRS}\rangle$, respectively, as far as the mechanism of HTSC is concerned, for which the relevant energy scale is expected to be smaller than 0.5 eV [3]. Note that the first-excited two-hole state is a spin-triplet (referred to as $|\text{axial}\rangle$) composed of one b_1 hole and one a_1 hole with excitation energy $\Delta_2 = 0.81$ eV for $\text{Ca}_2\text{CuO}_2\text{Cl}_2$, for example. A one-band model is thus obtained by projecting out all the other states by canonical perturbation and then mapping to a constrained fermion system without double occupancy [16].

Additional caution was paid to La_2CuO_4 . With a model tetragonal structure [2, 18, 19], we obtain $\varepsilon_{P_z} - \varepsilon_{P_s} = -0.52$ eV and Δ_2 is merely 0.13 eV, suggesting that a two-band Hamiltonian including $|\text{axial}\rangle$ be more appropriate. For this subtle case, other more realistic considerations are important; for example, we find that the 5° octahedral-tilting in the real material increases $\varepsilon_{P_z} - \varepsilon_{P_s}$ by 0.25 eV and Δ_2 by 100%. Such a tilting effect is interesting, as the oxygen dopants in $\text{Bi}_2\text{Sr}_2\text{CaCu}_2\text{O}_{8+\delta}$ also induce the tilting of nearby oxygen octahedra. To account for such effects, we present in Table I the results for the model La_2CuO_4 with $\varepsilon_{P_z} - \varepsilon_{P_s}$ being simply increased by 0.8 eV (now $\Delta_2 = 0.5$ eV); the ε_{P_z} effects are still large though considerably abated.

Results and Discussion.—The resulting effective one-band t - J -like Hamiltonian is given by [20]

$$\begin{aligned}
 H^{1b} = & - \sum_{ij\sigma} t_{ij} (\tilde{c}_{i\sigma}^\dagger \tilde{c}_{j\sigma} + H.c.) + J \sum_{\langle ij \rangle} (\vec{S}_i \cdot \vec{S}_j - \frac{n_i n_j}{4}) \\
 & + \frac{J}{4} \sum_{\langle ijk \rangle \sigma} (\tilde{c}_{i\sigma}^\dagger \tilde{c}_{j\bar{\sigma}}^\dagger \tilde{c}_{j\sigma} \tilde{c}_{k\bar{\sigma}} - \tilde{c}_{i\sigma}^\dagger n_{j\bar{\sigma}} \tilde{c}_{k\sigma} + H.c.) \\
 & + \sum_{\langle ij \rangle} V_{ij} n_i n_j + \sum_i \mu_i n_i + \sum_{ij} \varepsilon_{ij}, \quad (1)
 \end{aligned}$$

where $\tilde{c}_{i\sigma}$ is the annihilation operator for the constrained fermion with spin σ at site i . $n_{i\sigma} = \tilde{c}_{i\sigma}^\dagger \tilde{c}_{i\sigma}$, $n_i = \sum_\sigma n_{i\sigma}$, and $\vec{S}_i = \sum_{\mu\nu} \tilde{c}_{i\sigma}^\dagger \vec{\sigma}_{\mu\nu} \tilde{c}_{i\bar{\sigma}}$ with $\vec{\sigma}_{\mu\nu}$ being the Pauli matrices. All the site pairs $\langle ij \rangle$ stand for nearest neighbors except t_{ij} extends to the third nearest neighbors (referred to as t''). Note that the first two lines of Eq. (1) resemble the t - J model mapped out from the one-band Hubbard model and have been extensively studied [21]. The other terms include

ε_{P_z} -dependent “super-repulsion” V_{ij} , site potential μ_i , and energy “constant” ε_{ij} .

The derived parameters for several prototypical cuprates upon hole doping are listed in Table I. For comparison, the contributions purely from the b_1 orbitals (from which ZRS is formed) are given inside the parentheses in Table I. Remarkably, *there exists practically no material dependence if only the b_1 orbitals are considered*. The universality for t and J survives inclusion of the a_1 orbitals, since they are solely determined by the b_1 orbitals, suggesting that the magnetic mechanism be responsible for the robustness of superconductivity among the cuprates.

More amazingly, the material dependence of these materials *almost entirely results from the influence of the apical P_z orbitals*; the other a_1 orbitals have negligible contributions as made clear from comparing all the cases with Nd_2CuO_4 . t' , t'' , V_{ij} , μ_i , and ε_{ij} all show strong material- (ε_{P_z} -) dependence [c.f. Fig. 2(a)]. First of all, three-site kinematical processes via virtual nearest-neighbor hoppings to the P_z orbital dramatically renormalize t' and t'' , as suggested in Ref. [14]. These modulations would seriously affect the mobility of hole quasiparticles and the shape of the Fermi surface, given that the nearest-neighbor hoppings of hole quasiparticles are suppressed by the antiferromagnetic spin correlation [21]. Note that $-t'/t$ is substantially smaller in La_2CuO_4 than in $\text{Ca}_2\text{CuO}_2\text{Cl}_2$, consistent with their observed diamond- and square-like Fermi surfaces, respectively [4, 5].

Quantitatively, our calculated values of $-t'/t$ for the above two compounds are considerably smaller than the widely used ones (~ 0.15 and 0.3 , respectively) estimated from fitting ARPES in the very lightly doped t - J model [4, 5, 6, 22]. Interestingly, the single-hole quasiparticle dispersions calculated with the present parameters for $A_2\text{CuO}_2X_2$ ($A=\text{Ca}, \text{Sr}$; $X=\text{F}, \text{Cl}$) in the self-consistent Born approximation (SCBA) [6] still agree well with available ARPES data [4], as shown in Fig. 2(b). This is because the dispersion is actually more sensitive to t''/t , which is consistent between ours and previous estimations. Moreover, the fitted values of t' and t''

were shown to depend sensitively on inclusion of the three-site hopping terms $\propto J/4$ [22]. Our first-principles derived Hamiltonian finally provides an unambiguous benchmark of these material-dependent parameters.

In sharp contrast, the “downfolded” LDA one-band led to a puzzling opposite trend ($-t'/t = 0.18$ for La_2CuO_4 and 0.12 for $\text{Ca}_2\text{CuO}_2\text{Cl}_2$) [2] that appears in contradiction with ARPES and our parameters. This is, however, not alarming, since t 's in Eq. (1) describes hoppings of ZRS (intersite swapping of the $|\text{ZRS}\rangle$ and $|\sigma\rangle$ states [7]), while the LDA t 's describes hopping of the single-particle LDA $|\sigma\rangle$ state. This intrinsic difference can be easily observed from Fig. 1(b) where EUHB and ELHB are shown to have *different* WS characters, an essential feature missed in the picture of the LDA one-band plus effective Hubbard interaction [2]. Clearly, building the strong many-body characteristics in first-principles approaches before the downfolding [18, 19], as presented here, is necessary for the low-energy physics of cuprates.

Next, the striking appearance of the unconventional “super-repulsion” V_{ij} originates from two-site kinematical processes as demonstrated in Fig. 3. For a purely one-band system in the large on-site repulsion limit [Fig. 3(a)], the virtual hoppings between two singly-occupied neighboring sites generate the well-known superexchange effect $-\frac{J}{2}n_{i\sigma}n_{j\bar{\sigma}}$. Given an extra fully-occupied orbital to be projected out (P_z in the present work), additional virtual kinematical processes give rise to three new spin-independent terms [$\propto v_{00}$, v_{10} , and v_{11} , see Fig. 3(b)-(d)] to the targeted one-band Hamiltonian, leading to $V_{ij} = 2v_{10} - v_{00} - v_{11}$, $\mu_i = 4(v_{00} - v_{10})$ and $\varepsilon_{ij} = -v_{00}$.

This new effective repulsion, V_{ij} (named “super-repulsion” in analog to superexchange), is *to be distinguished from direct Coulomb interaction*: Not only is V_{ij} controlled by ε_{P_z} , but also its virtual kinematical origin makes it less subject to the electronic screening. Besides, as presented in Fig. 2(c), V_{ij} rapidly increases as $|t'/t|$ decreases from Nd_2CuO_2 to La_2CuO_2 . Therefore, for any realistic study of the cuprates, the V_{ij} effect should be addressed along with the t' effect.

As for superconductivity, the repulsive V_{ij} apparently

TABLE I: Derived parameters of Eq. (1) for four prototypical cuprates upon hole doping. Inside the parentheses are contributions purely from the b_1 orbitals. The energy unit is meV.

	Nd_2CuO_4	$\text{Sr}_2\text{CuO}_2\text{F}_2$	$\text{Ca}_2\text{CuO}_2\text{Cl}_2$	La_2CuO_4
T_c^{max} (K)	N/A	46	28	38
$\varepsilon_{P_z} - \varepsilon_{P_s}$	∞	3010	810	280 ^a
$J_{\text{LDA}+U}^b$	131	155	145	144
$J/2$	138 (138)	138 (138)	131 (131)	129 (129)
t	431 (431)	467 (467)	459 (459)	488 (488)
$t'/ t $	-0.33 (-0.35)	-0.25 (-0.32)	-0.19 (-0.32)	0.01 (-0.30)
$t''/ t $	0.23 (0.24)	0.19 (0.23)	0.16 (0.23)	0.06 (0.22)
V_{ij}	29 (27)	39 (29)	54 (30)	137 (31)
μ_i	-795 (-800)	-337 (-394)	-295 (-412)	-354 (-529)
ε_{ij}	-36 (-14)	-86 (-17)	-133 (-17)	-258 (-19)

^aIncreased by 0.8 eV (see text).

^bEstimated from total energies of the (anti)ferromagnetic states.

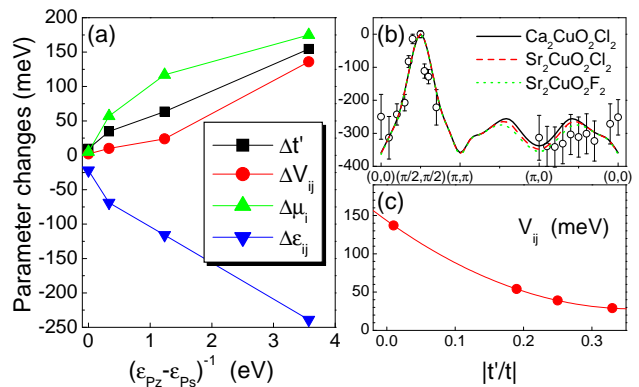


FIG. 2: (a) Parameter changes by the a_1 orbitals as a function of ε_{P_z} . (b) Calculated one-hole quasiparticle dispersions compared with ARPES on $\text{Sr}_2\text{CuO}_2\text{Cl}_2$ (open circles) [4]. (c) V_{ij} versus $|t'/t|$.

weakens the local pairing strength, regardless of the actual pairing mechanism, given that paired holes tend to reside as nearest neighbors (implied by the $d_{x^2-y^2}$ -wave symmetry of the order parameter [23]). This provides a natural avenue for modulating the local superconducting gap [11] as well as T_c . On the other hand, the suggested trend of $T_c^{\max} \sim t'/t$ [2, 14]—which turned out to be controversial in several numerical studies [24, 25, 26]—is clearly violated by comparing $\text{Ca}_{2-x}\text{Na}_x\text{CuO}_2\text{Cl}_2$ ($T_c^{\max}=28$ K) with $\text{La}_{2-x}\text{Sr}_x\text{CuO}_4$ ($T_c^{\max}=38$ K). It is thus fair to speculate that the full material dependence of T_c^{\max} involves other complex aspects of real materials (e.g., sample cleanness, doping approaches, two-band scenarios). Further investigation is needed to identify those aspects that affect T_c^{\max} beyond our present discovery.

With regard to charge distribution (CD), modulation of μ_i tends to induce charge inhomogeneity. As shown in Fig. 2(a), μ_i depends strongly on the apical environment. This explains strong *interlayer* charge inhomogeneity in multilayer systems such as $\text{HgBa}_2\text{Ca}_{n-1}\text{Cu}_n\text{O}_{2n+2+\delta}$ with $n \geq 3$ [27] and atomically perfect $\text{La}_{1.85}\text{Sr}_{0.15}\text{CuO}_4/\text{La}_2\text{CuO}_4$ films [28], as μ_i in distinct CuO_2 layers can be considerably different. On the other hand, repulsive V_{ij} , which disfavors hole accumulation, effectively counters μ_i to give a smoother *in-plane* CD.

The present results would shed new light on the understanding of other exotic features of cuprates. For example, recent SI-STM experiments on $\text{Bi}_2\text{Sr}_2\text{CaCu}_2\text{O}_{8+\delta}$ indicated that local superconducting gaps vary from 20 – 70 meV correlating with oxygen dopants, O_δ , *while* low-energy charge density variations are weak [11]. These striking results have been phenomenologically attributed to a strong local modulation of electron pairing strength [29], J in the t - J model [30], or μ_i with two types of O_δ [31]. The present studies suggest that O_δ perturb O_{apical} and thus significantly modulate V_{ij} , instead of J , in addition to μ_i , t' , and t'' . This new scenario also agrees well with more recent SI-STM measurements that

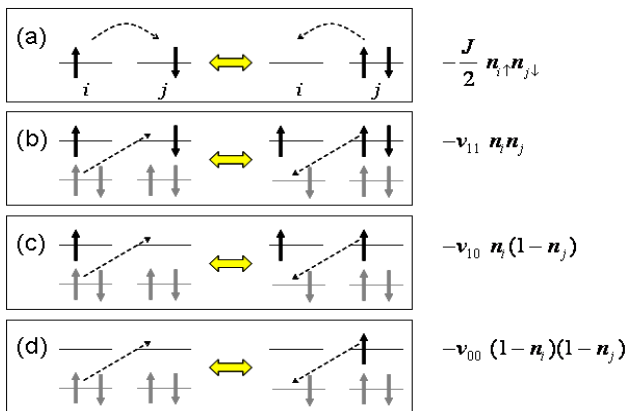


FIG. 3: Schematics of virtual kinematical processes and corresponding effective one-band interaction terms for (a) Heisenberg superexchange within a one-orbital system and (b)-(d) additional “vacuum fluctuations” in a two-orbital system. Electrons (solid arrows) in the targeted and projected orbitals are black and gray, respectively. Dashed lines denote hopping paths.

reveal a strong correlation between the local superconducting gap and $\text{Cu-O}_{\text{apical}}$ distance [12].

Furthermore, the strong ε_{P_z} dependence of t' , t'' , V_{ij} , and μ_i implies the electron-phonon interactions involving vibration of the apical atoms may be strong. In particular, the V_{ij} variation in this way yields an unconventional higher-order electron-phonon interaction. The determination of their actual strengths will be pursued elsewhere. The enhanced electron-phonon interactions could cooperate with V_{ij} in favoring other competing orders such as “stripe,” especially in doped La_2CuO_4 [32] where we have shown that the pair-breaking V_{ij} is comparable to J .

Finally, our findings point to the importance of examining HTSC in multi-layer systems [27, 33] or cuprate superlattices [28], as the influence of the apical P_z orbitals will be significantly layer-dependent and can be controlled (e.g., via strain and field effects) to tune hole concentration, mobility, and super-repulsion among the CuO_2 layers, a very interesting problem for future investigation.

We are grateful to S.R. White for his advice on numerical canonical transformation [34]. We thank J.C. Davis for presenting us SI-STM results [12] prior to publication. Helpful discussions with O.K. Andersen, P.W. Anderson, I. Bozovic, T.K. Lee, D.C. Mattis, W. E. Pickett, T.M. Rice, G. Sawatzky, R. Scalettar, A.M. Tselik, and Z. Wang are also acknowledged. This work was supported by US DOE (DE-AC02-98CH10886) and DOE-CMSN.

-
- [1] A. Cho, *Science* **314**, 1072 (2006).
 - [2] E. Pavarini, I. Dasgupta, T. Saha-Dasgupta, O. Jepsen, and O. K. Andersen, *Phys. Rev. Lett.* **87**, 047003 (2001).
 - [3] P. W. Anderson, P. A. Lee, M. Randeria, T. M. Rice, N. Trivedi, and F. C. Zhang, *J. Phys.: Condens. Matter* **16**, R755 (2004).
 - [4] A. Damascelli, Z.-X. Shen, and Z. Hussain, *Rev. Mod. Phys.* **75**, 473 (2003).
 - [5] K. Tanaka, T. Yoshida, A. Fujimori, D. H. Lu, Z.-X. Shen, X.-J. Zhou, H. Eisaki, Z. Hussain, S. Uchida, Y. Aiura, et al., *Phys. Rev. B* **70**, 092503 (2004).
 - [6] W.-G. Yin, C.-D. Gong, and P. W. Leung, *Phys. Rev. Lett.* **81**, 2534 (1998).
 - [7] F. C. Zhang and T. M. Rice, *Phys. Rev. B* **37**, 3759 (1988).
 - [8] Related discussions can be found in M. V. Mostovoy and D. I. Khomskii, *Phys. Rev. Lett.* **92**, 167201 (2004).
 - [9] W.-G. Yin, D. Volja, and W. Ku, *Phys. Rev. Lett.* **96**, 116405 (2006).
 - [10] W. Ku, H. Rosner, W. E. Pickett, and R. T. Scalettar, *Phys. Rev. Lett.* **89**, 167204 (2002).
 - [11] K. McElroy, J. Lee, J. A. Slezak, D.-H. Lee, H. Eisaki, S. Uchida, and J. C. Davis, *Science* **309**, 1048 (2005).
 - [12] J. C. Davis, unpublished.
 - [13] We applied the WIEN2k [P. Blaha *et al.*, *Comput. Phys. Commun.* **147**, 71 (2002)] implementation of the full potential linearized augmented plane wave method in the LDA+ U approach with $U = 8$ eV and $J = 0.88$ eV [V.I. Anisimov *et al.*, *Phys. Rev. B* **70**, 172501 (2004) and references therein].
 - [14] R. Raimondi, J. H. Jefferson, and L. F. Feiner, *Phys. Rev. B* **53**, 8774 (1996).

- [15] D. C. Mattis, Phys. Rev. Lett. **74**, 3676 (1995).
- [16] T. Kostyrko, Phys. Rev. B **40**, 4596 (1989).
- [17] The strong material dependence of ε_{P_z} was also found in the classic ionic model [Y. Ohta, T. Tohyama, and S. Maekawa, Phys. Rev. B **43**, 2968 (1991)].
- [18] A. K. McMahan, R. M. Martin, and S. Satpathy, Phys. Rev. B **38**, 6650 (1988).
- [19] M. S. Hybertsen, E. B. Stechel, M. Schluter, and D. R. Jennison, Phys. Rev. B **41**, 11068 (1990).
- [20] Small corrections of three-site hopping terms including $c_i^\dagger(1 - n_j)c_k$ have been neglected.
- [21] E. Dagotto, Rev. Mod. Phys. **66**, 763 (1994).
- [22] T. Xiang and J. M. Wheatley, Phys. Rev. B **54**, R12653 (1996).
- [23] C. C. Tsuei and J. R. Kirtley, Rev. Mod. Phys. **72**, 969 (2000).
- [24] S. R. White and D. J. Scalapino, Phys. Rev. B **60**, R753 (1999).
- [25] T. Maier, M. Jarrell, T. Pruschke, and J. Keller, Phys. Rev. Lett. **85**, 1524 (2000).
- [26] C. T. Shih, T. K. Lee, R. Eder, C.-Y. Mou, and Y. C. Chen, Phys. Rev. Lett. **92**, 227002 (2004).
- [27] H. Mukuda, M. Abe, Y. Araki, Y. Kitaoka, K. Tokiwa, T. Watanabe, A. Iyo, H. Kito, and Y. Tanaka, Phys. Rev. Lett. **96**, 087001 (2006).
- [28] I. Bozovic, G. Logvenov, M. A. J. Verhoeven, P. Caputo, E. Goldobin, and T. H. Geballe, Nature **422**, 873 (2003).
- [29] T. S. Nunner, B. M. Andersen, A. Melikyan, and P. J. Hirschfeld, Phys. Rev. Lett. **95**, 177003 (2005).
- [30] J.-X. Zhu, cond-mat/0508646.
- [31] S. Zhou, H. Ding, and Z. Wang, Phys. Rev. Lett. **98**, 076401 (2007).
- [32] J. M. Tranquada, H. Woo, T. G. Perring, H. Goka, G. D. Gu, G. Xu, M. Fujita, and K. Yamada, Nature **429**, 534 (2004).
- [33] Y. Chen, A. Iyo, W. Yang, X. Zhou, D. Lu, H. Eisaki, T. P. Devereaux, Z. Hussain, and Z.-X. Shen, Phys. Rev. Lett. **97**, 236401 (2006).
- [34] S. R. White, J. Chem. Phys. **117**, 7472 (2002).